

Targeted regulation of transcription in primary cells using CRISPRa and CRISPRi

Trine I. Jensen,¹ Nanna S. Mikkelsen,¹ Zongliang Gao,¹ Johannes Foßelteder,² Gabriel Pabst,² Esben Axelgaard,¹ Anders Laustsen,¹ Saskia König,¹ Andreas Reinisch,³ and Rasmus O. Bak^{1,4}

¹Department of Biomedicine, Aarhus University, 8000 Aarhus C., Denmark; ²Division of Hematology, Department of Internal Medicine, Medical University of Graz, 8010 Graz, Austria; ³Division of Hematology, Department of Internal Medicine and Department of Blood Group Serology and Transfusion Medicine, Medical University of Graz, 8010 Graz, Austria; ⁴Aarhus Institute of Advanced Studies, Aarhus University, 8000 Aarhus C., Denmark

Targeted transcriptional activation or interference can be induced with the CRISPR-Cas9 system (CRISPRa/CRISPRi) using nuclease-deactivated Cas9 fused to transcriptional effector molecules. These technologies have been used in cancer cell lines, particularly for genome-wide functional genetic screens using lentiviral vectors. However, CRISPRa and CRISPRi have not yet been widely applied to ex vivo cultured primary cells with therapeutic relevance owing to a lack of effective and nontoxic delivery modalities. Here we develop CRISPRa and CRISPRi platforms based on RNA or ribonucleoprotein (RNP) delivery by electroporation and show transient, programmable gene regulation in primary cells, including human CD34⁺ hematopoietic stem and progenitor cells (HSPCs) and human CD3⁺ T cells. We show multiplex and orthogonal gene modulation using multiple sgRNAs and CRISPR systems from different bacterial species, and we show that CRISPRa can be applied to manipulate differentiation trajectories of HSPCs. These platforms constitute simple and effective means to transiently control transcription and are easily adopted and reprogrammed to new target genes by synthetic sgRNAs. We believe these technologies will find wide use in engineering the transcriptome for studies of stem cell biology and gene function, and we foresee that they will be implemented to develop and enhance cellular therapeutics.

[Supplemental material is available for this article.]

The CRISPR-Cas9 gene editing system has been repurposed for precise transcriptional regulation of target genes by fusing catalytically disabled Cas9 (dCas9) to transcriptional modulators such as the tripartite transactivator VP64, p65, and Rta (VPR) or the transcriptional repressor Krüppel-associated box (KRAB) (Gilbert et al. 2013, 2014; Chavez et al. 2015). The dCas9 fusion complex is directed to the transcriptional start site (TSS) region of a target gene by Watson–Crick base-pairing between the associated single guide RNA (sgRNA) and the target locus (Fig. 1A).

CRISPR activation or inhibition (CRISPRa/i) has been shown to be highly specific and efficient in human cell lines and in vivo, where most studies have used either plasmids or various viral vectors to deliver the two components (Forstnerič et al. 2019; Black et al. 2020; Di Maria et al. 2020). However, CRISPRa/i in ex vivo cultured primary cells is more challenging because of the low plasmid transfection rates and high toxicity caused by intact DNA-sensing mechanisms (Genovese et al. 2014; Hendel et al. 2015). Lentiviral vectors have been widely used in cell lines and in some primary cell types, particularly for CRISPRa/i screens, but induce persistent transcriptional effects owing to chromosomal integration, which may not always be desirable for ex vivo applications (Gilbert et al. 2014; Savell et al. 2019).

The aim of this study was to develop transient RNA- and protein-based platforms that support efficient and nontoxic CRISPRa/i in primary cells, including CD34⁺ hematopoietic stem and pro-

genitor cells (HSPCs) and T cells. We believe that such platforms would constitute significant improvements over conventional plasmid-based delivery, not only with respect to toxicity but also in terms of efficiency.

Results

Exploring RNA-based delivery for CRISPRa in the K562 cell line.

We first produced in vitro transcribed (IVT) mRNA of the *Streptococcus pyogenes* dCas9-VPR and set up a range of CRISPRa experiments targeting genes encoding various cluster of differentiation (CD) cell surface proteins to allow single-cell expression analyses by flow cytometry. First, we performed a dose escalation matrix experiment in the K562 cell line to determine the optimal amounts of dCas9-VPR mRNA and two chemically modified sgRNAs directed at the TSS region of the *CXCR4* gene. Analysis of the *CXCR4* expression by flow cytometry showed very efficient gene activation at doses comparable to those used in previous conventional gene editing studies (Supplemental Fig. 1A; Bak et al. 2018). Next, we performed a direct comparison of plasmid-based and RNA-based CRISPRa of the *CXCR4* and *CD5* genes, both of which are not expressed in K562 cells. Plasmid-based electroporations were performed at optimized conditions (see Methods). Reverse transcription quantitative PCR (RT-qPCR) results showed

Corresponding author: bak@biomed.au.dk

Article published online before print. Article, supplemental material, and publication date are at <https://www.genome.org/cgi/doi/10.1101/gr.275607.121>.

© 2021 Jensen et al. This article is distributed exclusively by Cold Spring Harbor Laboratory Press for the first six months after the full-issue publication date (see <https://genome.cshlp.org/site/misc/terms.xhtml>). After six months, it is available under a Creative Commons License (Attribution-NonCommercial 4.0 International), as described at <http://creativecommons.org/licenses/by-nc/4.0/>.

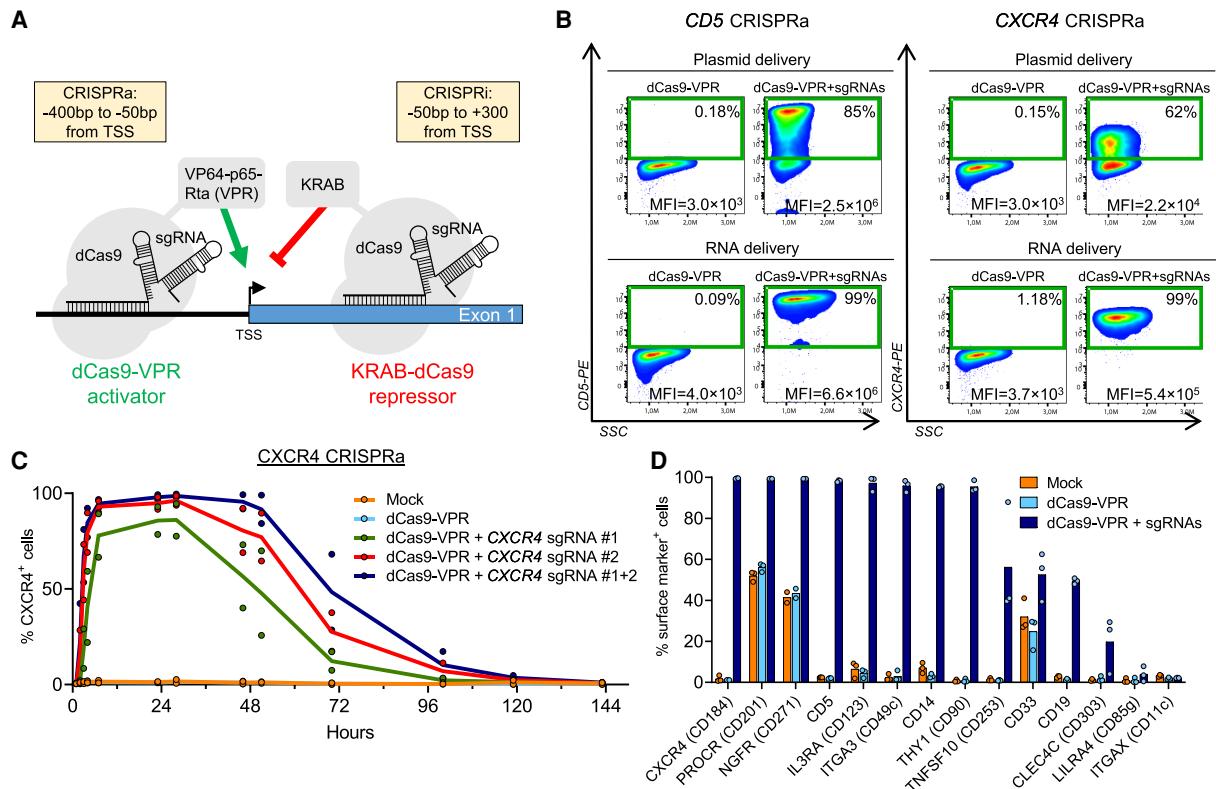


Figure 1. CRISPRa by plasmid and RNA-based delivery. (A) CRISPRa or CRISPRi is mediated by a nuclease-deactivated Cas9 (dCas9) fused to effector domains that either activate (VP64-p65-Rta [VPR]) or inhibit (KRAB) transcription. The fusion protein is guided by one or more sgRNAs targeted to the region surrounding the transcriptional start site (TSS). The guidelines for sgRNA positioning relative to the TSS have been empirically devised by Gilbert et al. (2014) and are shown in the yellow boxes. (B) Representative FACS plots (N = 3) showing the analyses of target gene expression in K562 cells 24 h after electroporation with CRISPRa systems based on either plasmid or RNA delivery. For the plasmid-based platform, one plasmid encodes dCas9-VPR, and separate plasmids each express a sgRNA targeting the TSS region of the target gene (*CD5* or *CXCR4*). The RNA-based platform is based on in vitro transcribed mRNA encoding dCas9-VPR and synthetic, chemically modified sgRNAs. Four sgRNAs were used for *CD5*, and two sgRNAs were used for *CXCR4*. Gates contain cells that are positive for the target protein with percentages shown in the upper right corner. Each FACS plot also displays the mean fluorescence intensity (MFI) of all live cells. (C) Time course experiment showing the percentage of CXCR4⁺ cells measured by flow cytometry following electroporation with dCas9-VPR mRNA and two chemically modified sgRNAs. (D) CRISPRa of 14 different target genes in K562 cells. Cells were analyzed by flow cytometry 24 h after electroporation with dCas9-VPR mRNA and chemically modified sgRNAs (two to four sgRNAs per gene). The percentage of cells positive for the surface marker is shown. For all graphs, N is number of data points, and all bars show mean values with individual data points plotted.

robust mRNA induction for both systems, with no statistical difference for *CD5* activation, whereas *CXCR4* activation was 7.9-fold higher for RNA-based delivery compared with plasmid (Supplemental Fig. 1B). Analysis by flow cytometry confirmed these results, but the single-cell nature of these analyses revealed a notable difference in the percentage of cells, in which the genes were activated. Although plasmid-based delivery gave rise to an average of 58.9% CXCR4⁺ cells and 86.6% CD5⁺ cells, RNA-based delivery gave rise to an average of 99.5% and 98.2% positive cells, respectively (Fig. 1B; Supplemental Fig. 1C). In addition, the levels of gene activation in the cell populations were much more homogenous following RNA-based delivery.

Next, we analyzed the kinetics of *CXCR4* CRISPRa in K562 cells following RNA-based delivery. Rapid gene activation was observed, with 50% of the cells expressing CXCR4 3 h after electroporation, reaching full activation after 7 h. Full gene activation lasted 48 h after which it declined to baseline 5–6 d after electroporation (Fig. 1C; Supplemental Fig. 1D). When delivering just one of the two *CXCR4*-targeting sgRNAs, we observed lower levels of activation and shorter activation duration, confirming prior studies showing the possibility of tuning these parameters with sgRNA selection (Strezoska et al. 2020).

We expanded the studies to 14 genes in total and observed near-full gene activation (>90% of cells expressing the gene) for eight target genes, partial activation of five genes, and no activation of one gene (Fig. 1D; Supplemental Fig. 1E). The inability to activate the *ITGAX* gene was confirmed by different means: (1) *ITGAX* antibody functionality was confirmed in PBMCs; (2) a different cell line (NALM-6) was tested (Supplemental Fig. 1F); (3) six additional *ITGAX* TSS-targeting sgRNAs were tested in K562 cells (Supplemental Fig. 1F); and (4) the functionality of all 10 *ITGAX* sgRNAs was confirmed by gene editing experiments with nuclease-active Cas9 showing 50%–94% indels in K562 cells (Supplemental Fig. 1G; Supplemental File 1). This supports prior studies showing that not all genes are amenable to CRISPRa (Alda-Catalinas et al. 2020). We also conclude from the data from these 14 genes that dCas9-VPR mRNA delivery alone without sgRNAs does not give rise to gene activation.

Several CRISPRa systems have been engineered, including the SAM system, which was previously reported to be as potent as, and in some instances more potent than, the VPR system (Chavez et al. 2016). The SAM system is based on the dCas9-VP64 fusion protein where additional activation is mediated by two more transcriptional activators that are brought to the dCas9-VP64 complex by

MS2 aptamer-carrying sgRNAs. The MS2 aptamers are recognized by the MS2 binding protein, which is fused to the two activators P65 and HSF1. Hence, the system is more complex than the VPR system because two separate proteins must be expressed, namely, dCas9-VP64 and MS2-P65-HSF1. Furthermore, the sgRNAs have two MS2 aptamers embedded into the stem loops, thereby extending the sgRNA to 160 nt. This is larger than current chemical RNA synthesis allows, which is necessary to include chemically modified nucleotides for optimal performance when delivered along mRNA (Hendel et al. 2015). However, an optimized chemically modified two-part guide RNA (gRNA) system is commercially available, in which the crRNA and MS2-carrying tracrRNA (SAM tracrRNA) must be annealed before delivery. We therefore produced dCas9-VP64 and MS2-P65-HSF1 mRNAs and codelivered these into K562 cells by electroporation along annealed SAM tracrRNAs and crRNAs targeting *CXCR4*. We compared this system to our existing VPR system at equivalent molar doses that were either half or double of what was previously used in dCas9-VPR experiments to better probe differences between the systems at suboptimal conditions and to investigate efficiencies at increased doses. Furthermore, experiments were performed using both *CXCR4*-targeting gRNAs (#1 + 2) for optimal performance or only the inferior gRNA (#1) for suboptimal performance. Across all conditions, these experiments showed much higher activation levels for the VPR system. When using twice the amount of the reagents than found optimal for the VPR system along both *CXCR4* gRNAs, the SAM system was only able to activate *CXCR4* expression in an average of 52% of the cells compared with 97% for the VPR system (Supplemental Fig. 2). At half the optimal dose, the VPR system was still able to activate *CXCR4* in 97% of the cells, whereas the SAM system showed activation in a modest 10.0% of cells. Hence, we conclude that in this experimental context, the VPR system is both simpler and more potent than the SAM system, and we therefore proceeded with the VPR system.

So far, CRISPRa experiments were performed with a combination of sgRNAs, so next we tested the performance of four individual sgRNAs targeting each of the genes *CD5*, *ITGA3*, *IL3RA*, and *NGFR*, which are expressed by <20% of K562 cells. Except for a single *CD5*-targeting sgRNA, all individual sgRNAs gave rise to potent CRISPRa with >75% of cells expressing the target gene (Fig. 2A). For all four genes, there was no marked difference in the percentage of cells with CRISPRa, but the activation levels based on mean fluorescence intensity (MFI) of all cells were highest when all four sgRNAs were combined.

The CRISPR-Cas9 system is easily reprogrammed and multiplexed to target several genes by combining multiple synthetic sgRNAs. To investigate if we could target several genes for multiplexed CRISPRa, we targeted the *CD5*, *ITGA3*, *IL3RA*, and *NGFR* genes simultaneously with either 1, 2, 3, or all four sgRNAs per target gene. In general, multiplexing 2 or 3 of the most potent sgRNAs per target gene yielded the best activation with the four genes being expressed by 72%–93% of all cells (Fig. 2B).

CRISPRa in CD34⁺ HSPCs and T cells

To explore the capacity of the RNA-based CRISPRa system to activate gene expression in human primary cells, we electroporated CD34⁺ HSPCs with dCas9-VPR mRNA and sgRNAs targeting either *CD5*, *CD14*, *ITGA3*, *THY1*, or *NGFR*. All five genes were efficiently activated with averages of 85%–96% of cells expressing the target protein (Fig. 3A; Supplemental Fig. 3A). To validate that CD34⁺ HSPCs subjected to CRISPRa retained stem cell properties, we targeted *PROCR* for CRISPRa and observed efficient up-regulation to >94% *PROCR*⁺ cells 24 h after electroporation (Supplemental Fig. 3B). The cells were then transplanted into irradiated immunodeficient mice and 20 wk after transplantation, we observed multilineage human engraftment in the bone marrow, confirming the

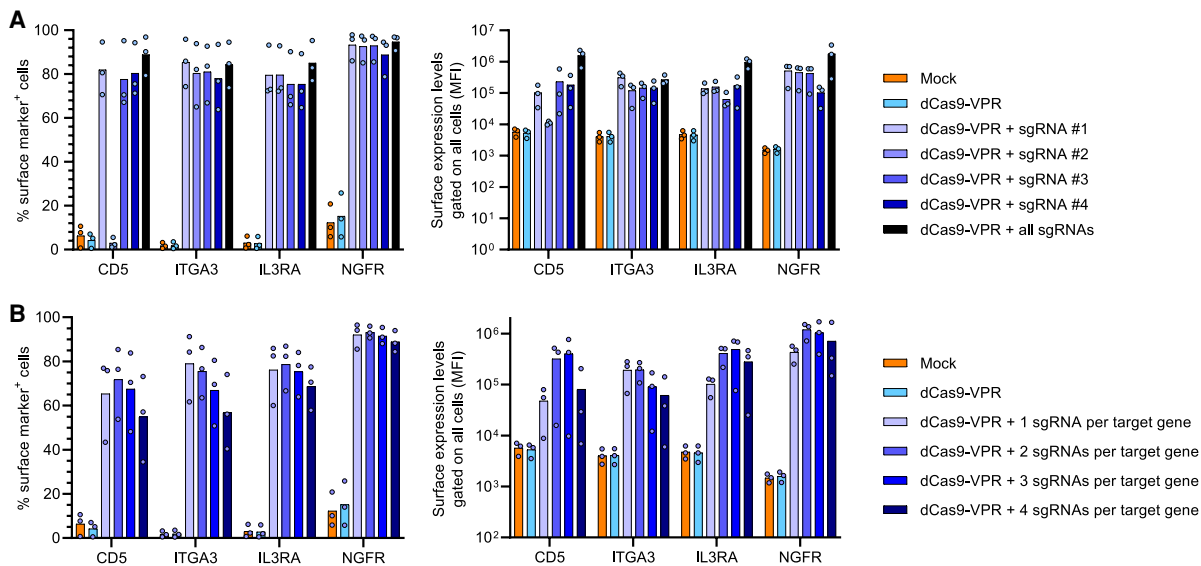


Figure 2. Activity of individual sgRNAs and multiplexed CRISPRa. (A) K562 cells were electroporated with dCas9-VPR mRNA and one of four individual sgRNAs targeting the TSS region of the genes *CD5*, *ITGA3*, *IL3RA*, and *NGFR*. The percentages of surface marker–positive cells (left) and the MFI of all live cells (right) were determined 24 h after electroporation by flow cytometry. (B) Multiplexed CRISPRa was investigated by electroporating K562 cells with dCas9-VPR mRNA and one, two, three, or all sgRNAs per target gene. sgRNA combinations were selected based on decreasing potency from the experiment shown in A; that is, when a single sgRNA was used for each gene, this was the most potent sgRNA as identified in A. The percentage of surface marker–positive cells (left) and the MFI of all live cells (right) were determined 24 h after electroporation by flow cytometry. For all graphs, N is the number of data points. All bars show mean values with individual data points plotted.

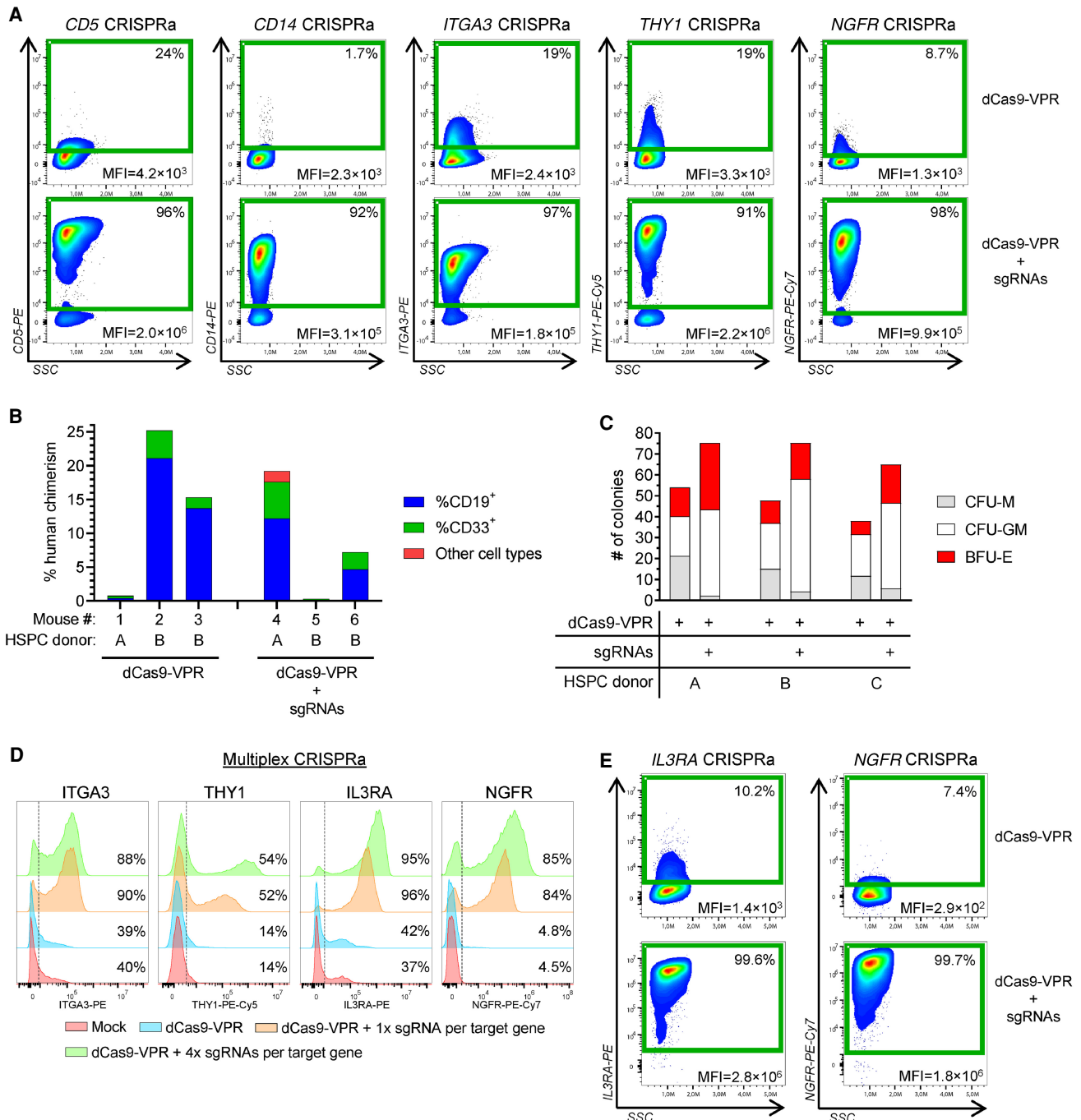


Figure 3. CRISPRa in human CD34⁺ HSPCs. (A) CRISPRa in human CD34⁺ HSPCs electroporated with dCas9-VPR mRNA and chemically modified sgRNAs (three to four sgRNAs per gene). Representative FACS plots are shown with the gates containing surface marker–positive cells 24 h post electroporation and the frequencies of cells within the gates are shown. Each FACS plot also displays the MFI of all live cells. (B) To confirm maintained repopulation potential of human CD34⁺ HSPCs following CRISPRa, CD34⁺ HSPCs from two cord blood donors (A and B) were electroporated with dCas9-VPR mRNA with or without three chemically modified sgRNAs targeting *PROCR* and then transplanted into irradiated immunodeficient NOG mice. Twenty weeks after transplant, bone marrow of the transplanted mice was analyzed by flow cytometry for human chimerism and multilineage reconstitution (CD33⁺ myeloid cells and CD19⁺ B cells). Graphs show the percentage of human chimerism for individual mice with the fraction of myeloid cells, lymphoid cells, and other cell types shown within each bar. Each bar represents one mouse. (C) Colony-forming unit (CFU) assay of CD34⁺ HSPCs from three donors with or without CRISPRa of the *GATA1* gene. HSPCs were seeded in semisolid methylcellulose media 24 h after electroporation, and colonies were counted and scored 14 d after. (CFU-M) Monocyte colonies, (CFU-GM) granulocyte/macrophage colonies, (BFU-E) burst-forming unit erythroid colonies. (D) Multiplex CRISPRa in human CD34⁺ HSPCs with simultaneous gene activation of four different surface markers. Representative FACS histograms show surface marker expression 24 h after electroporation with dCas9-VPR mRNA and chemically modified sgRNAs (one or four sgRNAs per gene). The vertical dashed lines indicate the threshold for gating marker–positive cells. (E) CRISPRa in primary human T cells. Representative FACS plots show surface marker expression 24 h after electroporation with dCas9-VPR mRNA and chemically modified sgRNAs (four sgRNAs per gene). All FACS plots are representative, and the number of replicates and donors used are shown in the associated data presented in Supplemental Figures 3 through 5.

presence of primitive stem cells with long-term repopulation potential (Fig. 3B; Supplemental Fig. 3C).

To exemplify a functional application of CRISPRa, we next sought to manipulate the lineage output during HSPC differentiation. GATA1 is a master transcription factor that acts during hematopoiesis to direct differentiation of erythroid, megakaryocytes, and nonneutrophilic granulocytes (Nei et al. 2013; Drissen et al. 2016). We therefore performed a colony-forming unit (CFU) assay of CD34⁺ HSPCs electroporated with *GATA1*-targeting sgRNAs and dCas9-VPR mRNA. Intracellular flow cytometry confirmed activation of *GATA1*, which was expressed in >80% of the cells compared with ~10% without CRISPRa (Supplemental Fig. 4A). Assessment of colony output showed an average of a 54% increase in total colony numbers as well as a strong bias toward BFU-E (erythroid) and CFU-GM (granulocyte-macrophage) colonies for the *GATA1*-activated population (Fig. 3C; Supplemental Fig. 4B). We also observed a significant suppression of generated CFU-M (monocytes). These results align with previous studies using lentiviral *GATA1* delivery to murine bone marrow cells, showing that *GATA1* overexpression increases clonogenic efficiency with ~50% and leads to a significant increase in erythroid and nonneutrophilic granulocyte differentiation at the expense of monocyte differentiation (Nerlov et al. 2000; Heyworth et al. 2002). A time course analysis of *GATA1* mRNA and protein levels in the CRISPRa condition showed rapid induction of *GATA1* mRNA, which was observable 2 h after electroporation and peaked at the 8-h time point (Supplemental Fig. 4C,D). As expected, protein expression was delayed relative to mRNA expression with detectable activation 4–8 h post-electroporation, peaking at 24 h. *GATA1* mRNA and protein levels declined only slowly for the 9-d duration of the experiment but are confounded by natural *GATA1* induction with the onset of erythroid and myeloid differentiation.

We next performed multiplexed CRISPRa of four genes in CD34⁺ HSPCs (*ITGA3*, *THY1*, *IL3RA*, and *NGFR*). We used either one sgRNA per target gene or four sgRNAs per target gene. These experiments showed potent multiplexed activation of *ITGA3*, *IL3RA*, and *NGFR* with >86% surface marker-positive cells for all three genes across three HSPC donors, whereas *THY1* activation was observed in an average of 61% of cells (Fig. 3D; Supplemental Fig. 5A). When comparing one or four sgRNAs per target gene, we did not observe any notable difference in the percentage of cells in which the four genes were activated, but the levels of activation based on MFI were higher for *THY1* and *NGFR* when using four sgRNAs (Supplemental Fig. 5A).

We also tested CRISPRa of *IL3RA* and *NGFR* in activated primary human T cells and observed efficient induction of gene expression from <30% to >99% of cells expressing the genes following CRISPRa (Fig. 3E; Supplemental Fig. 5B). In murine cell lines (NIH/3T3 fibroblasts and EL4 T cells) and in activated primary murine T cells, efficient CRISPRa was also observed when targeting the *Ccr7* gene (Supplemental Fig. 5C).

CRISPRa by RNP delivery

State-of-the-art CRISPR-Cas9 *ex vivo* gene editing of CD34⁺ HSPCs is performed with electroporation of Cas9 protein complexed with sgRNAs (ribonucleoprotein [RNP]), which performs better than RNA-based delivery (Dever et al. 2016). We therefore explored the possibility of delivering dCas9-VPR using RNPs but were unable to obtain recombinant dCas9-VPR protein from *Escherichia coli*. However, recombinant dCas9-VP64 was produced at high yields, and we therefore performed a comparison of RNA- and RNP-based

CRISPRa despite the effector molecules not having the same transcriptional activation potency (plasmid-based experiments have shown a 22- to 320-fold improved activation of VPR over VP64) (Chavez et al. 2015). CRISPRa of the *PROCR*, *CXCR4*, or *CD5* genes in CD34⁺ HSPCs gave rise to gene activation in >90% of the cells for both systems, but as expected owing to the less potent effector molecule, the activation levels were significantly lower for the RNP-based CRISPRa system (Fig. 4A; Supplemental Fig. 6A). Analysis of activation kinetics for *CD5* CRISPRa showed similar durations of activation for both systems with activation in >80% of cells observed from 24 h to 5 d after electroporation and returning to baseline 6–7 d after electroporation (Supplemental Fig. 6B,C).

CRISPRi and orthogonal transcriptional engineering

Next, we explored RNA-based delivery for CRISPRi. We first electroporated K562 cells with KRAB-dCas9 mRNA along chemically modified sgRNAs targeting the TSS region of the *PROCR* gene. Three sgRNAs, either delivered individually or combined, decreased the frequency of cells expressing *PROCR* from ~35% to 0.6%–2% (Supplemental Fig. 7A,B). We then tested *CD5* gene repression in primary human T cells, which all express CD5 at very high levels (>99%). Kinetic analyses showed that CRISPRi had a slower onset than CRISPRa, but nearly full silencing (94%–95% of cells with complete gene silencing) was observed 5 d post electroporation (Fig. 4B; Supplemental Fig. 8). At 6–11 d post electroporation, CD5 expression slowly increased to 77% CD5⁺ cells, after which a fraction of the cells adopted a CD5-negative phenotype, possibly reflecting intrinsic *CD5* regulatory mechanisms.

We finally investigated orthogonal transcriptional regulation combining CRISPRa and CRISPRi for different genes (Supplemental Fig. 9A). To ensure orthogonality, each of the dCas9-effector molecules (dCas9-VPR and KRAB-dCas9) must not complex with the sgRNAs intended for the other dCas9-effector. We therefore first established CRISPRa using the CRISPR-Cas9 system from *Staphylococcus aureus* (Sa), which complexes to sgRNAs with unique scaffolds and uses a PAM sequence different from SpCas9. CRISPRa with dSaCas9-VPR proved effective for activating *NGFR* and *CXCR4* in the K562 cell line (Supplemental Fig. 9B). In studies of CRISPRa of *CXCR4*, we included both unmodified and modified sgRNAs, which gave rise to 2.8% and 96% of cells expressing *CXCR4*, respectively, thereby confirming previous studies showing that chemical modifications to the sgRNA are essential for activity of an RNA-based CRISPR-Cas9 system (Hendel et al. 2015). We then investigated simultaneous activation of *CXCR4* using dSaCas9-VPR and repression of *PROCR* using KRAB-dSpCas9 in K562 cells. Despite CRISPRa and CRISPRi not being kinetically aligned, we investigated if it would be feasible to use a single electroporation of all components, which would simplify the workflow of orthogonal transcriptional engineering. These results showed that an average of 83% of all cells displayed full simultaneous *CXCR4* activation and full *PROCR* repression 3 d post electroporation and returned to baseline around day 10 (Fig. 4C; Supplemental Fig. 10). Similar experiments in primary human T cells with orthogonal regulation of *NGFR* (CRISPRa) and *CD5* (CRISPRi) showed an average of 69% of all cells with full simultaneous *NGFR* activation and *CD5* repression 5 d post electroporation (Fig. 4D; Supplemental Fig. 11A,B). The effect gradually decreased for both genes, with most cells reaching baseline at ~2 wk following electroporation (Supplemental Fig. 11A,B). To evaluate potential toxicity of the CRISPRa+i treatment, T cell numbers were tracked throughout the experiment and showed no difference

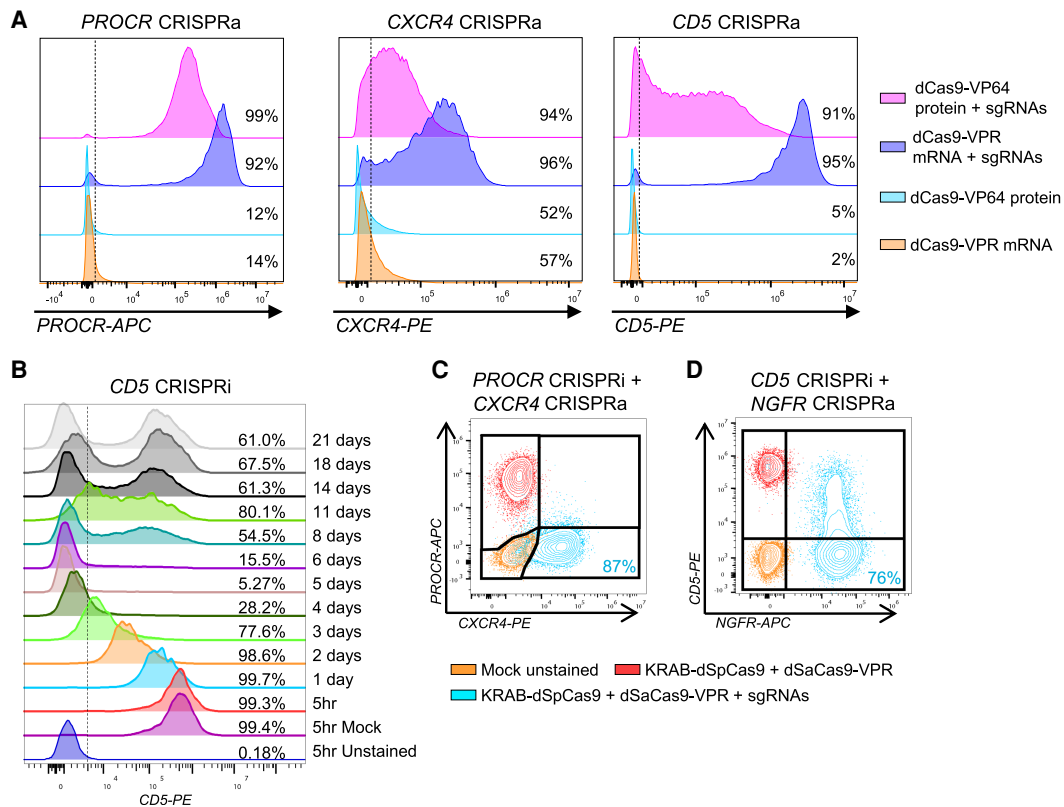


Figure 4. CRISPRa by RNP delivery and CRISPRi for orthogonal gene regulation. (A) Comparison of RNP- and RNA-based delivery for CRISPRa of *PROCR*, *CXCR4*, or *CD5*. CD34⁺ HSPCs were electroporated with dCas9-VPR mRNA and chemically modified sgRNAs or dCas9-VP64 protein precomplexed with chemically modified sgRNAs. Representative FACS histograms show expression levels of the target genes 24 h after electroporation as well as frequencies of surface marker-positive cells. The vertical dashed lines represent the gate for surface marker expression. All plots are representative, and the number of replicates and donors used are shown in the associated data presented in Supplemental Figure 6. (B) Time course experiment of CRISPRi in primary human T cells. Cells were electroporated with KRAB-dCas9 mRNA and three chemically modified sgRNAs targeting the TSS region of *CD5*. *CD5* expression was analyzed by flow cytometry at the indicated time points. The vertical dashed line indicates the threshold for marker-positive cells. (C) Orthogonal transcriptional gene regulation in K562 cells by electroporation with KRAB-dSpCas9 mRNA and three sgRNAs targeting the TSS region of *PROCR* (CRISPRi) together with dSaCas9-VPR mRNA and two sgRNAs targeting the TSS region of *CXCR4* (CRISPRa). The overlay FACS plot shows analysis at day 3 post electroporation of an unstained mock sample (orange), a stained sample only receiving the two mRNAs (red), and a stained sample receiving the two mRNAs and sgRNAs (blue). For the orthogonal CRISPRa + i condition (blue), the percentage of cells in the lower right quadrant is shown in blue. (D) Orthogonal transcriptional gene regulation in primary human T cells performed as in C, but instead targeting *CD5* (CRISPRi) and *NGFR* (CRISPRa). All plots are representative, and the number of replicates and donors used are shown in the associated data presented in Supplemental Figures 8, 10, and 11.

between mock treatment and orthogonal CRISPRa + i, showing that the treatment was well tolerated (Supplemental Fig. 11C).

Discussion

Here we show robust, efficient, and homogenous activation and repression of target genes in primary hematopoietic cells, which traditionally have been difficult to manipulate. A comparison between plasmid and RNA-based delivery showed a clear advantage of RNA over plasmid, in particular when measuring CRISPRa on a per-cell basis using flow cytometry. In contrast to RT-qPCR, single-cell analysis was able to uncover very heterogeneous gene activation when using plasmid delivery. With RNA-based delivery, it was evident that transfection efficiencies approached 100%, leading to a very homogenous gene activation. Prior studies have shown that plasmids are toxic to many primary cells, including CD34⁺ HSPCs, and are not a viable approach for genome engineering of these cells (Genovese et al. 2014; Hendel et al. 2015). Furthermore, plasmid DNA can be genomically integrated, which could lead to sustained CRISPRa/i activity in a subset

of cells, which may be undesirable and may even cause severe adverse effects in a therapeutic setting. In terms of off-target activity, several prior studies have found CRISPRa and CRISPRi to be highly specific (Chavez et al. 2016; Matharu et al. 2019; Savell et al. 2019). In contrast to gene editing with nuclease-active Cas9, CRISPRa and CRISPRi effectors are only active within narrow windows around TSSs, and if an off-target site should exist at a TSS, the risk of sustained adverse effects would expectedly be low because no permanent changes are made to the genome.

We showed rapid onset of CRISPRa within the first 24 h after electroporation, whereas CRISPRi displayed slower kinetics with full effect reached within 3–5 d post electroporation. Durations were variable but were, in general, confined to a few days, which is likely to be gene and cell type dependent. Longer durations might be obtained by repeated electroporations if necessary, but the very transient nature of these delivery methods should be highly attractive, for example, in studies of stem cell differentiation to briefly activate transcriptional networks that induce a new cellular state. We show this by lineage reprogramming of HSPCs by transcriptional engineering with CRISPRa.

In general, we observed little to no toxicity from RNA- or RNP-based delivery. After electroporation, human T cells expanded to the same extent as mock-treated cells, and HSPCs retained their capacity to engraft long-term in immunodeficient mice. However, these transplantation studies were performed with only three mice per group and did not include mock-treated cells. Because this transplantation model is known to be prone to high variations, exemplified by the presented data, we cannot rule out any positive or negative impact on repopulation from CRISPRa or from being exposed to the CRISPRa reagents. In fact, prior studies have observed some decrease in repopulation capacity of Cas9 mRNA-treated HSPCs, and Cas9 mRNA has been shown to induce innate immune responses and global transcriptional down-regulation in metabolic and cell cycle processes (Dever et al. 2016; Cromer et al. 2018).

We showed that both magnitude and duration of activation could be tuned by careful sgRNA selection, which adds a layer of control to the platform. It may also be possible to tune the system by changing properties of the dCas9-effector mRNA such as poly(A) tail length, codon usage, and incorporation of modified nucleotides. We were somewhat surprised that mRNA and RNP delivery were comparable in terms of activation duration. Both delivery modalities displayed a fast onset of CRISPRa, which is in line with gene editing observations comparing Cas9 mRNA and Cas9 RNP delivery (Liang et al. 2015). However, RNP delivery gave rise to gene activation for >5 d post electroporation. Prior reports have shown that Cas9 RNP is cleared from the cells after 24–48 h (Kim et al. 2014). Hence, our observations might indicate that the dCas-VP64 protein has higher intracellular stability compared with Cas9 and/or that the targeted CD5 protein has a long half-life. Further studies should determine whether RNP delivery gives rise to shorter durations of CRISPRa for other genes, which might offer an additional way of tuning the platform.

Most tested target genes were amenable to both CRISPRa and CRISPRi, but a few genes showed partial or no gene activation. This corroborates previous data from a pooled lentiviral CRISPRa screen using two sgRNAs for each of 230 genes (Alda-Catalinas et al. 2020). Here, single-cell RNA-seq from almost 204,000 cells expressing a unique sgRNA showed that only 49.6% of sgRNAs activated the cognate gene. The proportion of active sgRNAs is higher in our study, which might be owing to RNA delivery being more potent than lentiviral delivery, as has been shown previously (Strezoska et al. 2020). However, we were not able to induce *ITGAX* gene expression despite testing 10 different sgRNAs scattered within a 495-bp window from –633 bp to –138 bp relative to the TSS. The sgRNAs were selected based on previously optimized design algorithms derived from comprehensive machine learning trained on chromatin accessibility features, position, and sequence features from pooled sgRNA screens (Horlbeck et al. 2016; Sanson et al. 2018). The algorithms rely on the FANTOM Consortium-annotated TSSs (The FANTOM Consortium and the RIKEN PMI and CLST [DGT] 2014), which are considered the most reliable source of TSS annotations (Radzisheuskaya et al. 2016). Hence, we hypothesize that strong inhibitory epigenetic effects prevent induced activation of *ITGAX*, but also we note that other factors could cause or contribute to this. For example, genes that display differential translation rates through microRNAs or mRNA-binding regulatory proteins may respond differently to CRISPRa/i, and feedback mechanisms that control gene expression may also impact the efficiency and dynamics of CRISPRa/i. Future studies should address these questions and why some genes are apparently refractory to transcriptional regulation.

Historically, most genetic perturbation studies have been performed in laboratory-adapted, easy-to-manipulate cell lines that may not be related to the tissue of interest. Furthermore, cancer cell lines display high genomic instability, and the genetic pathway of interest might be inactive or have lost its natural regulation. Hence, a transition to primary cells will facilitate more relevant and reliable results. Cas9 mRNA and chemically modified sgRNA delivery by electroporation have shown very high gene editing efficiencies in a wide array of human cell types such as pluripotent stem cells, mesenchymal stromal cells, human neural stem cells, and NK cells (Dever et al. 2019; Martin et al. 2019; Pomeroy et al. 2020; Srifa et al. 2020). Hence, the presented CRISPRa/i platforms should also find wide applicability in many different cell types beyond those used in the current study.

With the ability to engineer transcription directly in the primary cells of interest with high efficiency and precision, we expect this platform to be relevant to studies of fundamental cell biology and characterization of gene function. The system is based on nonviral delivery and facilitates very effective targeted gene regulation in almost all treated cells without any antibiotic selection. The platform is particularly easy to adopt in laboratories not previously acquainted with the technology, and it can effortlessly be reprogrammed to new target genes by commercially available synthetic sgRNAs. Compared with cDNA delivery approaches, RNA-based CRISPRa/i benefits from being cloning-free, and it induces or represses expression of all isoforms transcribed from a promoter. It is highly scalable and easily implemented for arrayed CRISPRa/i screens as has previously been described (Strezoska et al. 2020). Additionally, transcriptional engineering may find use in cellular therapeutics and regenerative medicine to direct cell differentiation to a specific lineage or to enhance specific cell functions.

Methods

Plasmid constructs

Plasmids for in vitro mRNA transcription were based on a backbone containing the T7 promoter with the AG initiator, allowing cotranscriptional capping with CleanCap reagent AG from TriLink. The stop codon of the GOI is followed by the 93-bp 3' UTR of the murine *Hba-a1* gene, then a stretch of 50 adenines (poly(A)), and finally a unique restriction site that is not present anywhere else in the region from the T7 promoter to the poly(A). The GOIs were as follows: dSpCas9-VPR amplified from Addgene plasmid 63798 (a gift from George Church), KRAB-dSpCas9 amplified from Addgene plasmid 85449 (a gift from Eric Lander), dSaCas9-VPR amplified from Addgene plasmid 68495 (a gift from George Church), dCas9-VP64 amplified from Addgene plasmid 75112 (a gift from Feng Zhang), and MS2-p65-HSF1 amplified from Addgene plasmid 89308 (a gift from Feng Zhang). Primers contained compatible overhangs with the backbone for Gibson cloning. Primer sequences are listed in Supplemental Table 1. sgRNA expression plasmids were constructed by cloning annealed oligonucleotides containing 20-bp spacer sequences (with additional G at first position if not already present) and compatible overhangs into either SapI-digested Addgene plasmid 85451 (a gift from Hetian Lei) or a variant of Addgene plasmid 42230 (a gift from Feng Zhang), in which CMV-Cas9 was deleted by XbaI/EcoRI digestions followed by Klenow end-filling and ligation. All plasmid sequences were confirmed by Sanger sequencing. Oligonucleotide sequences are listed in Supplemental Table 1.

In vitro transcription

All IVT mRNAs were generated by T7 RNA polymerase run-off IVT of plasmids linearized with a restriction enzyme cutting immediately after the poly(A). Following plasmid linearization, 3 μ L of the digestion reaction was run on a 1% agarose gel to verify successful linearization. The linearized plasmid was precipitated with 5 M ammonium acetate and ethanol to concentrate and purify the DNA and subsequently used as template in the IVT reaction. IVT was performed using the MEGAscript kit (Ambion, Thermo Fisher Scientific) according to the instruction manual, but with full substitution of uridine with pseudouridine (TriLink Biotechnologies or APExBio) and cotranscriptional capping with CleanCap AG (TriLink Biotechnologies) in a 1:4 ratio between GTP and CleanCap. The mRNA was purified and concentrated using the RNA Clean & Concentrator kit (Zymo Research) according to the instruction manual. The quality of the IVT RNA was confirmed on a denaturing formaldehyde gel and quantified by UV-Vis spectrophotometry.

Recombinant Cas9-VP64 production

The recombinant Cas9-VP64 protein was produced in *E. coli* by the QB3 Macrolab at the University of California, Berkeley, according to the previously published protocol by Lingeman et al. (2017) with the following modifications: A 5 mL HiTrap heparin HP column was used instead of a 5 mL HiTrap SP HP column, and the gradient for elution was from 10%–100% ion exchange buffer B over 12 CV. After the size-exclusion step, the pooled fractions were filtered through an endotoxin-binding filter (Mustang E, 0.2 μ M, Pall Life Sciences) and then concentrated to \sim 40 μ M (6.4 mg/mL) before being aliquoted.

sgRNAs

All sgRNAs were acquired from Synthego as chemically modified sgRNAs containing 2'-O-methyl groups at the three first and last bases and 3' phosphorothioate bonds between the first three and the last two bases. Chemically modified and synthetic tracrRNA (Edit-R SAM tracrRNA) and crRNAs (custom Edit-R crRNA) were purchased from Horizon Discovery. Spacer sequences are listed in Supplemental Table 2. sgRNA design guidelines have previously been devised by Gilbert et al. (2014). Here, sgRNAs for CRISPRa should be designed to bind between -400 and -50 bp upstream of the TSS of the endogenous target gene, and for CRISPRi experiments, sgRNAs should be designed to bind between -50 and $+300$ bp relative to the TSS, with peak activity in the region 50 – 100 bp just downstream from the TSS. Most of the sgRNAs used in our studies were extracted from the CRISPRa and CRISPRi libraries devised by Horlbeck et al. (2016) and Sanson et al. (2018), with at least 30 bp between adjacent protospacer sequences to the extent possible.

Cell culture

K562 and NALM-6 cells were cultured in RPMI-1640 medium and 3T3 and EL4 cells in DMEM. Media was supplemented with 10% heat-inactivated FCS, 2 mM L-glutamine, 100 U/mL penicillin, and 100 μ g/mL streptomycin. HSPCs were acquired from umbilical cord blood. First, mononuclear cells were extracted using Ficoll-Paque plus density gradient, and then CD34⁺ cells were purified by immunomagnetic positive selection with the EasySep human cord blood CD34 positive selection kit II (StemCell Technologies). CD34⁺ HSPCs were cultured in SCGM media (CellGenix) containing 20 μ g/mL streptomycin, 20 U/mL penicillin, recombinant human SCF (100 ng/mL, Peprotech), human TPO (100 ng/mL,

Peprotech), recombinant human Flt3-L (100 ng/mL, Peprotech), StemRegenin 1 (0.75 μ M, StemCell Technologies), and UM171 (35 nM, StemCell Technologies). For retaining stemness throughout pre-expansion before electroporation, HSPCs were cultured at a cell density of 10^5 – 5×10^5 cells/mL. Primary human T cells were purified using immunomagnetic negative selection with the EasySep human T cell isolation kit (StemCell Technologies) starting from PBMCs isolated by Ficoll-Paque plus density gradient. Human T cells were cultured in X-VIVO 15 media (Lonza) supplemented with 5% human serum (Merck), 100 IU/mL IL2 (Peprotech), and 10 ng/mL IL7 (Peprotech). Cells were activated for 3 d with Dynabeads human T-activator CD3/CD28 (Thermo Fisher Scientific) at a 1:1 cell-to-bead ratio and reactivated for 3 d when deemed necessary (at \sim 7–10 d after the initial activation). For counting human T cells to generate a proliferation graph, cells were counted on a Bio-Rad TC20 cell counter using trypan blue to eliminate dead cells from the count. Each cell population was counted twice, and the average was used. Splenic murine T cells were isolated from Swiss Webster mice (Taconic) using immunomagnetic negative selection with the MojoSort mouse CD3 T cell isolation kit (BioLegend) on PBMCs isolated by Ficoll-Paque plus density gradient. Cells were cultured in RPMI 1640 medium GlutaMAX supplement, HEPES (Gibco, Thermo Fisher Scientific) supplemented with MEM nonessential amino acids at 1 \times (Gibco, Thermo Fisher Scientific), 50 μ M β -mercaptoethanol, 1 mM sodium pyruvate, 10% heat-inactivated FCS, 2 mM L-glutamine, 100 U/mL penicillin, 100 μ g/mL streptomycin, and 100 IU/mL human IL2 (Peprotech). Before electroporation, cells were activated for 3 d with Dynabeads mouse T-activator CD3/CD28 (Thermo Fisher Scientific) at a 1:1 cell-to-bead ratio.

Electroporations

All cells were electroporated using the 4D-nucleofector device form Lonza (Core and X unit), either in 20- μ L-format Nucleocuvette strips or 100- μ L-format Nucleocuvettes. Cells were electroporated with the following electroporation buffers and programs: murine EL4 cells—Opti-MEM, CM120-P3; murine 3T3 cells—Opti-MEM, CM183-P3; primary murine T cells—P3 primary cell 4D-Nucleofector kit (Lonza), DN100-P3; NALM-6 cells—OptiMEM, CM138-P3; primary human T cells—solution 1 M (Bak et al. 2018), EO115-P3; human CD34⁺ HSPCs—solution 1 M (Bak et al. 2018), DZ100-P3; and K562 cells—Opti-MEM or electroporation buffer solution I+II (Bak and Porteus 2017), CM138-P3. Cell concentrations during electroporation were between 2.5×10^6 – 5×10^7 cells/mL.

For CRISPRa and CRISPRi RNA-based delivery experiments, unless otherwise specified, cells were electroporated with 95 μ g/mL mRNA + 50 μ g/mL of each of the sgRNAs. For comparison of the VPR and SAM system, half (0.5 \times reagents) or double (2 \times reagents) of these amounts were used for the VPR condition. Equal molar amounts of the mRNAs and (s)gRNAs were used for these comparisons; that is, if X mole dCas9-VPR mRNA was used in the VPR condition, then X mole of dCas9-VP64 mRNA + X mole of MS2-P65-HSF1 mRNA was used in the SAM condition. Likewise, if Y mole of sgRNA was used for the VPR condition, then Y mole of gRNA (complexed crRNA:tracrRNA at a 1:1 ratio) was used for the SAM condition.

For multiplex experiments, dCas9-VPR mRNA concentration was kept fixed at 95 μ g/mL while adding sgRNAs each at 50 μ g/mL final concentration. For simultaneous (orthogonal) CRISPRa and CRISPRi experiments, cells were electroporated with 95 μ g/mL dCas9-VPR mRNA and 95 μ g/mL KRAB-dCas9 mRNA and each sgRNA at 50 μ g/mL.

For RNP-based delivery, the RNP complexes were formed by mixing dCas9-VP64 protein and sgRNA for 15 min at room temperature followed by incubation at 4°C until electroporation. Separate RNP complexes were formed for each sgRNA. RNP complexes were mixed with cells resuspended in electroporation buffer. The final concentrations in the electroporation solution were 450 µg/mL dCas9-VP64 protein + 240 µg/mL sgRNA per RNP complex. For plasmid-based delivery, cells were electroporated with the molar ratio between the dCas9-VPR plasmid and sgRNA-expressing plasmids used in Chavez et al. (2015). We set up optimization experiments testing escalating plasmid concentrations from 4 µg/mL to 62.5 µg/mL dCas9-VPR plasmid (with fixed ratio to the sgRNA-expressing plasmids) and determined the optimal amount to be 25 µg/mL dCas9-VPR plasmid + 1.7 µg/mL of each sgRNA plasmid in the final electroporation solution. For gene editing of *ITGAX* with nuclease-active Cas9 protein, Cas9 and sgRNA were mixed and incubated for 15 min at room temperature followed by storage at 4°C until electroporation. RNP complexes were then mixed with cells resuspended in electroporation buffer. The final concentrations during electroporations were 320 µg/mL Cas9 protein (IDT, Alt-R S.p. Cas9 Nuclease V3) and 160 µg/mL sgRNA (Synthego; see below for further information on sgRNAs). Genomic DNA was extracted using QuickExtract DNA extraction solution (Lucigen) 4 d post electroporation. The *ITGAX* genomic region containing the sgRNA target sites were PCR-amplified using the following primer pairs: Fw, 5'-TGGCCCTGACCTTGCTCTCTT-3'; Rv, 5'-CAGCCCTACTTCATTGGGGT-3'. The PCR products were gel-purified and Sanger-sequenced (Eurofin Genomics), and the AB1 sequencing files (Supplemental File 1) were analyzed using the ICE CRISPR analysis tool (Synthego) to quantify indel rates using a mock-electroporated sample as control.

Flow cytometry

To assess the CRISPRa and CRISPRi efficiencies, the expression of target genes was analyzed using flow cytometry. Briefly, between 1×10^5 and 2×10^5 cells were spun down, washed in PBS, and then resuspended in staining buffer (PBS, 2% FCS, 2 mM EDTA). Cells were stained with fluorochrome-conjugated antibodies (see Supplemental Table 3) for 30 min. After three washing steps in staining buffer, the fluorescence intensities were measured by flow cytometry either on a Novocyte analyzer (Agilent), Quanteon analyzer (Agilent), or LSR Fortessa (BD). For intracellular staining of GATA1, 2.5×10^5 cells were spun down and fixed with PBS containing 2% formaldehyde (EMS) for 10 min at 37°C. After washing in PBS, cells were permeabilized using Perm Buffer III (BD Biosciences) for 30 min on ice. Thereafter, cells were washed in staining buffer and incubated with a primary rabbit monoclonal anti-GATA1 antibody (Cell Signaling Technology, clone D52H6, 1:800) for 30 min at RT. After another washing step in staining buffer, cells were stained with a secondary antirabbit IgG-AF647 antibody (Cell Signaling Technology) for 30 min at RT. A final washing step in staining buffer was performed before fluorescence intensities were measured by flow cytometry on a CytoFLEX S instrument (Beckman Coulter). Data were analyzed using FlowJo, gating first on the primary cell population in an FSC/SSC plot, then excluding doublets using a FSC height/width plot, and then on live cells by using low-FSC cells outside the primary FSC/SSC gate as dead control cells, and finally, the surface marker-positive cells were gated using an unstained or isotype control sample.

Reverse transcription quantitative PCR

Gene expression levels of *CXCR4*, *CD5*, and *GATA1* were determined by RT-qPCR. Total RNA was extracted from cells using the

ReliaPrep RNA cell miniprep system (Promega; *CXCR4* and *CD5*) or Monarch total RNA miniprep kit (NEB; *GATA1*) according to manufacturer's protocol. Complementary DNA was synthesized from total RNA using a iScript reverse transcription supermix (Bio-Rad, *CXCR4* and *CD5*) or LunaScript RT supermix kit (NEB, *GATA1*) according to the supplied protocols. Quantitative PCR was performed using the Maxima probe/Rox qPCR master mix (Thermo Fisher Scientific) (*CXCR4* and *CD5*) or Luna universal qPCR master mix (NEB, *GATA1*). Probe-based qPCR was performed for *CXCR4* and *CD5* with a primer/probe mix against *CXCR4* (IDT, PrimeTime qPCR assay Hs.PT.58.27595676.g) or *CD5* (Thermo Fisher Scientific, TaqMan assay ID Hs00204397_m1). The analysis was performed on a LightCycler 480 (Roche) according to standard procedures. *RPLPO* was used as a housekeeping reference gene (IDT, PrimeTime qPCR assay Hs.PT.39a.22214824). For calculating relative levels of gene activation for plasmid- versus RNA-based delivery, the standard curve method was used using serially diluted cDNA from a CRISPRa sample, and target mRNA relative concentrations were normalized to *RPLPO* concentrations. These relative levels were then normalized to the plasmid delivery sample set to one. All RT-qPCR for *CXCR4* and *CD5* reactions were conducted in biological triplicates with each biological triplicate analyzed in technical triplicates during qPCR. For *GATA1*, an intercalating dye-based qPCR was performed on a QuantStudio 5 real-time PCR system (Applied Biosystems) with the following primers: *GATA1*—fwd 5'-CCACTACCTATGCAACGCCT-3', rev 5'-GC CCGTTTACTGACAATCAGG-3'; *B2M*—fwd 5'-CCACTGAAAAG ATGAGTATGCCT-3', rev 5'-CCAATCCAATGCGGCATCTTCA-3'; *ACTB*—fwd 5'-CACCATTGGCAATGAGCGGTTTC-3', rev 5'-AGGT CTTTGCGGATGTCCACGT-3'; and *HPRT1*—fwd 5'-TGAGGATT GGAAAGGGTGT-3', rev 5'-GAGCACACAGAGGGCTACAA-3'. *GATA1* and housekeeping gene expression was measured from two biological samples with each two technical replicates. *GATA1* mRNA expression was normalized to the three housekeeping genes and then to the 0-h time point using the $\Delta\Delta CT$ method. The mean fold change was then calculated from the normalization to the three housekeeping genes.

Methylcellulose colony-forming assay

Twenty-four hours after nucleofection with *GATA1* sgRNAs and dCas9-VPR mRNA or only with dCas9-VPR mRNA, 300 cells per 6-cm dish were plated in triplicates with semisolid methylcellulose medium (MethoCult, StemCell Technologies GFH84435). Cells were incubated for 14 d at 37°C, and colonies were counted and scored based on morphologic evaluation (colony-forming unit granulocyte/macrophage [CFU-GM], colony-forming unit monocyte [CFU-M], burst-forming unit erythroid [BFU-E]) according to the manual Human Colony-Forming Unit (CFU) Assays Using MethoCult from StemCell Technologies.

Transplantation of CD34⁺ HSPCs into immunodeficient NOG mice

Six- to 8-wk-old female CIEA NOG mice (NOD.Cg *Prkdc^{scid} Il2rg^{tm1Sug}/JicTac*) were purchased from Taconic Biosciences. One day after electroporation, 1×10^5 cells were administered by tail-vein injection after sublethal X-ray irradiation (75 cGy). Before transplantation, flow cytometry confirmed that >98% of HSPCs were CD34⁺. Mice were randomly assigned to each experimental group and evaluated in a blinded fashion.

Assessment of human engraftment

At week 20 post transplantation, mice were sacrificed, and bone marrow was collected by flushing femurs and tibiae with a 2-

gauge $\times 1/2''$ needle. Cells were then passed through a 100- μm cell strainer before being washed with PBS and then treated with red blood cell lysis buffer (eBioscience) for 10 min at RT followed by washing in ice-cold FACS buffer and centrifugation for 10 min at 300g at 4°C. Cells were blocked for nonspecific antibody binding (10% vol/vol, TruStain FcX, BioLegend) and stained (30 min, 4°C, dark) with the following antibodies: antihuman PTPRC (CD45, V450), antihuman CD19 (APC), antihuman CD33 (PE), antihuman HLA-A/B/C (APC-Cy7), antimouse PTPRC^a (CD45.1, PE-Cy7), and antimouse Ly76 (Ter119, PE-Cy5). Antibody clones and vendors are listed in Supplemental Table 3. Human engraftment was defined by the presence of cells positive for both PTPRC (CD45) and HLA-A/B/C.

Statistics

All *P*-values were calculated by a two-tailed Student's *t*-test to test the null hypothesis of no difference between the mean of the two compared groups. Equal variances were tested by an *F*-test. *P* < 0.05 was considered statistically significant.

Ethics statement

Informed consent to use cord blood–derived CD34⁺ HSPCs for experimental purposes was acquired from the mothers. At the Medical University of Graz, cord blood collections were approved by the Institutional Review Board (IRB; Ethikkommission, EK# 31322 ex 1819) of the Medical University of Graz IRB. Donor information was kept anonymized to all researchers. All animal studies were performed with permission from the Danish Experimental Animal Inspectorate.

Competing interest statement

R.O.B. holds equity in Graphite Bio. A.L. and R.O.B. hold equity in and are part-time employees of UNIKUM Therapeutics. The other authors declare that they have no competing interests.

Acknowledgments

We thank the FACS Core Facility at Aarhus University for providing invaluable help with flow cytometry and Niels Uldbjerg, Lars Henning Pedersen, and Hai Qing Tang from Aarhus University Hospital for consenting and procuring cord blood. We thank Pernille Thornild Møller for technical assistance. R.O.B. acknowledges the support from a Lundbeck Foundation fellowship (R238-2016-3349), the Independent Research Fund Denmark (0134-00113B, 0242-00009B, and 9144-00001B), an AIAS-COFUND (Marie Curie) fellowship from Aarhus Institute of Advanced Studies (AIAS) cofunded by Aarhus University's Research Foundation and the European Union's seventh Framework Program under grant agreement no. 609033, the Novo Nordisk Foundation (NNF19OC0058238 and NNF17OC0028894), Innovation Fund Denmark (8056-00010B), the Carlsberg Foundation (CF20-0424 and CF17-0129), Slagtermester Max Wørzner og Hustru Inger Wørzners Mindelegat, the AP Møller Foundation, the Riisfort Foundation, and a Genome Engineer Innovation grant from Synthego. Z.G. acknowledges support from an individual postdoctoral fellowship from the Lundbeck Foundation (R303-2018-3571).

Author contributions: T.I.J. and R.O.B. conceived the study and designed the experiments. T.I.J. performed experiments and analyses with assistance from N.S.M., Z.G., J.F., G.P., E.A., A.L., and S.K. All experiments were supervised by A.R. and R.O.B. T.I.J. and

R.O.B. wrote the manuscript with input from all coauthors. All authors reviewed and edited the final manuscript.

References

- Alda-Catalinas C, Bredikhin D, Hernando-Herraez I, Santos F, Kubinyecz O, Eckersley-Maslin MA, Stegle O, Reik W. 2020. A single-cell transcriptomics CRISPR-activation screen identifies epigenetic regulators of the zygotic genome activation program. *Cell Syst* **11**: 25–41.e9. doi:10.1016/j.cels.2020.06.004
- Bak RO, Porteus MH. 2017. CRISPR-mediated integration of large gene cassettes using AAV donor vectors. *Cell Rep* **20**: 750–756. doi:10.1016/j.celrep.2017.06.064
- Bak RO, Dever DP, Porteus MH. 2018. CRISPR/cas9 genome editing in human hematopoietic stem cells. *Nat Protoc* **13**: 358–376. doi:10.1038/nprot.2017.143
- Black JB, McCutcheon SR, Dube S, Barrera A, Klann TS, Rice GA, Adkar SS, Soderling SH, Reddy TE, Gersbach CA. 2020. Master regulators and cofactors of human neuronal cell fate specification identified by CRISPR gene activation screens. *Cell Rep* **33**: 108460. doi:10.1016/j.celrep.2020.108460
- Chavez A, Scheiman J, Vora S, Pruitt BW, Tuttle M, Iyer EPR, Lin S, Kiani S, Guzman CD, Wiegand DJ, et al. 2015. Highly efficient Cas9-mediated transcriptional programming. *Nat Methods* **12**: 326–328. doi:10.1038/nmeth.3312
- Chavez A, Tuttle M, Pruitt BW, Ewen-Campen B, Chari R, Ter-Ovanesyan D, Haque SJ, Cecchi RJ, Kowal EJK, Buchthal J, et al. 2016. Comparison of Cas9 activators in multiple species. *Nat Methods* **13**: 563–567. doi:10.1038/nmeth.3871
- Cromer MK, Vaidyanathan S, Ryan DE, Curry B, Lucas AB, Camarena J, Kaushik M, Hay SR, Martin RM, Steinfeld I, et al. 2018. Global transcriptional response to CRISPR/Cas9-AAV6-based genome editing in CD34⁺ hematopoietic stem and progenitor cells. *Mol Ther* **26**: 2431–2442. doi:10.1016/j.ymthe.2018.06.002
- Dever DP, Bak RO, Reinisch A, Camarena J, Washington G, Nicolas CE, Pavel-Dinu N, Saxena N, Wilkens AB, Mantri S, et al. 2016. CRISPR/cas9 β -globin gene targeting in human hematopoietic stem cells. *Nature* **539**: 384–389. doi:10.1038/nature20134
- Dever DP, Scharenberg SG, Camarena J, Kildebeck EJ, Clark JT, Martin RM, Bak RO, Tang Y, Dohse M, Birgmeier JA, et al. 2019. CRISPR/cas9 genome engineering in engraftable human brain-derived neural stem cells. *iScience* **15**: 524–535. doi:10.1016/j.isci.2019.04.036
- Di Maria V, Moindrot M, Ryde M, Bono A, Quintino L, Ledri M. 2020. Development and validation of CRISPR activator systems for overexpression of CB1 receptors in neurons. *Front Mol Neurosci* **13**: 168. doi:10.3389/fnmol.2020.00168
- Drissen R, Buza-Vidas N, Woll P, Thongjuea S, Gambardella A, Giustacchini A, Mancini E, Zriwil A, Lutteropp M, Grover A, et al. 2016. Distinct myeloid progenitor-differentiation pathways identified through single-cell RNA sequencing. *Nat Immunol* **17**: 666–676. doi:10.1038/ni.3412
- The FANTOM Consortium and the RIKEN PMI and CLST (DGT). 2014. A promoter-level mammalian expression atlas. *Nature* **507**: 462–470. doi:10.1038/nature13182
- Forstnerič V, Oven I, Ogorevc J, Lainšček D, Praznik A, Lebar T, Jerala R, Horvat S. 2019. CRISPRa-mediated *FOXP3* gene upregulation in mammalian cells. *Cell Biosci* **9**: 93. doi:10.1186/s13578-019-0357-0
- Genovese P, Schirotti G, Escobar G, Tomaso TD, Firrito C, Calabria A, Moi D, Mazzieri R, Bonini C, Holmes MC, et al. 2014. Targeted genome editing in human repopulating hematopoietic stem cells. *Nature* **510**: 235–240. doi:10.1038/nature13420
- Gilbert LA, Larson MH, Morsut L, Liu Z, Brar GA, Torres SE, Stern-Ginossar N, Brandman O, Whitehead EH, Doudna JA, et al. 2013. CRISPR-mediated modular RNA-guided regulation of transcription in eukaryotes. *Cell* **154**: 442–451. doi:10.1016/j.cell.2013.06.044
- Gilbert LA, Horlbeck MA, Adamson B, Villalta JE, Chen Y, Whitehead EH, Guimaraes C, Panning B, Ploegh HL, Bassik MC, et al. 2014. Genome-scale CRISPR-mediated control of gene repression and activation. *Cell* **159**: 647–661. doi:10.1016/j.cell.2014.09.029
- Hendel A, Bak RO, Clark JT, Kennedy AB, Ryan DE, Roy S, Steinfeld I, Lunstad BD, Kaiser RJ, Wilkens AB, et al. 2015. Chemically modified guide RNAs enhance CRISPR-Cas genome editing in human primary cells. *Nat Biotechnol* **33**: 985–989. doi:10.1038/nbt.3290
- Heyworth C, Pearson S, May G, Enver T. 2002. Transcription factor-mediated lineage switching reveals plasticity in primary committed progenitor cells. *EMBO J* **21**: 3770–3781. doi:10.1093/emboj/cdf368
- Horlbeck MA, Gilbert LA, Villalta JE, Adamson B, Pak RA, Chen Y, Fields AP, Park CY, Corn JE, Kampmann M, et al. 2016. Compact and highly active next-generation libraries for CRISPR-mediated gene repression and activation. *eLife* **5**: e19760. doi:10.7554/eLife.19760

- Kim S, Kim D, Cho SW, Kim J, Kim JS. 2014. Highly efficient RNA-guided genome editing in human cells via delivery of purified Cas9 ribonucleoproteins. *Genome Res* **24**: 1012–1019. doi:10.1101/gr.171322.113
- Liang X, Potter J, Kumar S, Zou Y, Quintanilla R, Sridharan M, Carte J, Chen W, Roark N, Ranganathan S, et al. 2015. Rapid and highly efficient mammalian cell engineering via Cas9 protein transfection. *J Biotechnol* **208**: 44–53. doi:10.1016/j.jbiotec.2015.04.024
- Lingeman E, Jeans C, Corn JE. 2017. Production of purified CasRNPs for efficacious genome editing. *Curr Protoc Mol Biol* **120**: 31.10.1–31.10.19. doi:10.1002/cpmb.43
- Martin RM, Ikeda K, Cromer MK, Uchida N, Nishimura T, Romano R, Tong AJ, Lemgart VT, Camarena J, Pavel-Dinu M, et al. 2019. Highly efficient and marker-free genome editing of human pluripotent stem cells by CRISPR-Cas9 RNP and AAV6 donor-mediated homologous recombination. *Cell Stem Cell* **24**: 821–828.e5. doi:10.1016/j.stem.2019.04.001
- Matharu N, Rattanasopha S, Tamura S, Maliskova L, Wang Y, Bernard A, Hardin A, Eckalbar WL, Vaisse C, Ahituv N. 2019. CRISPR-mediated activation of a promoter or enhancer rescues obesity caused by haploinsufficiency. *Science* **363**: eaau0629. doi:10.1126/science.aau0629
- Nei Y, Obata-Ninomiya K, Tsutsui H, Ishiwata K, Miyasaka M, Matsumoto K, Nakae S, Kanuka H, Inase N, Karasuyama H. 2013. GATA-1 regulates the generation and function of basophils. *Proc Natl Acad Sci* **110**: 18620–18625. doi:10.1073/pnas.1311668110
- Nerlov C, Querfurth E, Kulesa H, Graf T. 2000. GATA-1 interacts with the myeloid PU.1 transcription factor and represses PU.1-dependent transcription. *Blood* **95**: 2543–2551. doi:10.1182/blood.V95.8.2543
- Pomeroy EJ, Hunzeker JT, Kluesner MG, Lahr WS, Smeester BA, Crosby MR, Lonetree CL, Yamamoto K, Bendzick L, Miller JS, et al. 2020. A genetically engineered primary human natural killer cell platform for cancer immunotherapy. *Mol Ther* **28**: 52–63. doi:10.1016/j.ymthe.2019.10.009
- Radzishchanskaya A, Shlyueva D, Müller I, Helin K. 2016. Optimizing sgRNA position markedly improves the efficiency of CRISPR/dCas9-mediated transcriptional repression. *Nucleic Acids Res* **44**: e141. doi:10.1093/nar/gkw583
- Sanson KR, Hanna RE, Hegde M, Donovan KF, Strand C, Sullender ME, Vaimberg EW, Goodale A, Root DE, Piccioni F, et al. 2018. Optimized libraries for CRISPR-Cas9 genetic screens with multiple modalities. *Nat Commun* **9**: 5416. doi:10.1038/s41467-018-07901-8
- Savell KE, Bach SV, Zipperly ME, Revanna JS, Goska NA, Tuscher JJ, Duke CG, Sultan FA, Burke JN, Williams D, et al. 2019. A neuron-optimized CRISPR/dCas9 activation system for robust and specific gene regulation. *eNeuro* **6**: ENEURO.0495-18.2019. doi:10.1523/ENEURO.0495-18.2019
- Srifa W, Kosaric N, Amorin A, Jadi O, Park Y, Mantri S, Camarena J, Gurtner GC, Porteus M. 2020. Cas9-AAV6-engineered human mesenchymal stromal cells improved cutaneous wound healing in diabetic mice. *Nat Commun* **11**: 2470. doi:10.1038/s41467-020-16065-3
- Strezoska Z, Dickerson SM, Maksimova E, Chou E, Gross MM, Hemphill K, Hardcastle T, Perrett M, Stombaugh J, Miller GW, et al. 2020. CRISPR-mediated transcriptional activation with synthetic guide RNA. *J Biotechnol* **319**: 25–35. doi:10.1016/j.jbiotec.2020.05.005

Received April 5, 2021; accepted in revised form August 9, 2021.